ACS OMEGA

http://pubs.acs.org/journal/acsodf Article

Experimental Research on Enhanced Oil Recovery Methods for Gas Injection of Fractured Reservoirs Based on Microfluidic Chips

Xiangling Li, Kang Xiao,* Ruifeng Wang, and Xianbing Li

Cite This: *ACS Omega* 2022, 7, 27382−27389 Read Online

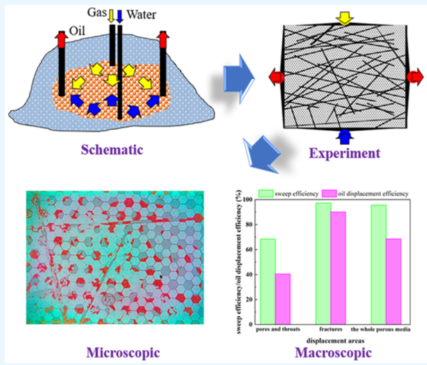

ABSTRACT: Gas injection is an effective method to enhance oil recovery of low-permeability and tight reservoirs, while the complicated fractures distributed in the formation have a noticeable effect on the performance of gas injection. In this study, three methods of gas injection were employed to conduct microfluidic experiments using micromodels simulating fractured reservoirs. The sweep efficiency and oil displacement efficiency of pores and throats, fractures, and the whole region were measured respectively to evaluate the oil displacement effects of the different gas injection methods. Moreover, the microscopic displacement process and the morphology of residual oil in porous media were analyzed to investigate the behavior of gas activated oil. The experimental results show that there are three stages of gas displacing oil: the oil in fractures was displaced first, then the oil in the pores and throats around the fracture was displaced, and finally the gas channeling occurred in fractures. Moreover, the sweep efficiency and oil displacement efficiency showed a tendency of increasing fast first and then reaching a steady state. Simultaneous injection of gas and water showed an optimal enhanced oil recovery effect among these three injection methods. Gas can invade deep throats, and those are difficult for water to sweep. However, the higher viscosity of water endowed it a smaller mobility than gas. And, the channeling in the two-phase mixing region was inhibited more obviously. The overall sweep efficiency and oil displacement efficiency increased about 18.4% and 13.4%, respectively.

1. INTRODUCTION

Low permeability and tight reservoirs play a significant role in the development of oil and gas reservoirs because of the huge reserves.[1−3] However, as a result of its small pores and throats, it is extremely difficult to develop compared with conventional reservoirs.[4−6] With the huge demand of economic and industrial development, expanding the scale of development and especially enhancing the development of low permeability and tight oil reservoirs is one of the urgent problems to be improved.[7,8] Fractures are ubiquitous in the reservoirs, especially in tight formations, such as the BachHo oilfield in Vietnam, the Yanling oilfield in China, the Baobab oilfield in Chad, etc.[9−11] In tight reservoirs, it is difficult for water to be injected as a result of smaller pore and throat size, which is detrimental to efficient development.[12−14] Compared with water, gas is easier to inject into a tight formation, making it a more suitable solution than water in tight reservoirs.[15,16] Among gas flooding methods, N_2 is impressively insoluble in water and chemically stable compared with hydrocarbon gas and CO_2. Additionally, N_2 has a small compressibility factor and is therefore not easily compressed. These characteristics endow N_2 with the ability to replenish the formation energy and maintain the formation pressure. N_2 flooding is considered to be an effective method to enhance oil recovery. However, fractured reservoirs are characterized by well-developed fractures, low matrix permeability, and high heterogeneity.[17−19] In addition, with the external and internal effects such as weathering for many years, the development degree of matrix and fractures in different parts of the reservoir from top to bottom is different, which further exacerbates the complexity and development difficulty of natural fractured reservoirs.[20−23] During the development process, the injected fluid channeling is prone to occur along fractures and high permeability areas, which makes it difficult to sweep the oil and reduce the ultimate oil recovery.[24,25] Due to high heterogeneity and structure complexity in naturally fractured reservoirs, the inhibition of gas channeling is challenging despite the existence of giant oil reserves in fractured reservoirs.[26,27]

Understanding gas flow behaviors in porous media is critical to exploring how to enhance oil recovery efficiently by gas flooding. Conn et al.[28] investigated the flow behaviors and the effect of foam on enhanced oil recovery by using a microfluidic

Received: April 17, 2022
Accepted: July 7, 2022
Published: July 26, 2022

https://doi.org/10.1021/acsomega.2c02390
ACS Omega 2022, 7, 27382−27389

chip with a wide central fracture. They clearly observed differences in the flow of gas through fractures, pores, and throats. Bai et al.[29] performed gas huff and puff experiments in fractured cores to study the effect of gas on residual oil distribution at fractures and areas with different permeability levels. It can be seen that the oil was primarily produced from the fractures and macropores, while the residual oil in the fractured cores was mainly distributed in small and medium pores and throats. Chen et al.[30] analyzed the effect of flue gas flooding on tight fractured reservoirs and the distribution of residual oil after gas flooding by a low-field nuclear magnetic resonance (LFNMR) system. They found that the existence of fractures in cores reduced the oil recovery significantly compared with a fracture-free core, playing a negative role in enhanced oil recovery of gas flooding in tight reservoirs. Zhang et al.[31] prepared a bulk gel by wormlike micelles generated from a CO_2-responsive smart mobility control system to mitigate serious gas channeling and low sweep efficiency of CO_2 gas flooding for enhanced oil recovery in ultralow permeability reservoirs. The experimental results showed that the fracture was blocked, and the CO_2 gas was diverted to the pores and throats to displace the residual oil. Although many scholars have previously carried out studies on the oil displacement characteristics of gas in fractured cores, almost all of them simulate the case of single-fracture cores, and there are still no reports on the visual study of the case of multiple fractures, pores, and throats at the same time. In particular, there is no previous study on gas flooding and gas−water coflooding in porous media with different development degrees of pores, throats, and fractures.

In this study, pore-scale flow behaviors of gas and the enhanced oil recovery method for gas injection of fractured reservoirs were explored by using microscopic visual porous media. The novel micromodels with pores and throats as well as a complex network of fractures were designed and fabricated to intuitively observe the pore-scale flow behaviors of gas. Moreover, this paper mainly discussed the effect of oil displacement in three types of porous media with different development degrees of pores, throats, and fractures by three gas injection methods. The optimal gas injection method for the development of fractured reservoirs was evaluated from macroscopic and microscopic perspectives.

2. EXPERIMENTAL SECTION

2.1. Materials. The experimental oil was offered by the Research Institute of Petroleum Exploration and Development (Beijing, China), with a viscosity of 12.5 mPa·s at room temperature (25 °C). Nitrogen gas (purity of >99.99%) was purchased from Beijing Jinggao Gas Co., Ltd., China. Ethanol and petroleum ether were used to wash the microfluidic chips and purchased from Shanghai Titan Scientific Co., Ltd., China. Deionized water was prepared for glass cleaning and oil displacement.

2.2. Methods. *2.2.1. Design and Preparation of Microfluidic Chips.* To clearly study the flow behaviors of gas in porous media simulating formation with fractures, three microfluidic chips are designed and fabricated, as shown in Figure 1a−c. The pores and throats of porous media are designed with regular shape, in which the pores are regular hexagons of equal size and the throats are narrow channels connecting vertexes of hexagons. The fractures are rectangular channels with random distribution. The size of the porous media area in the microfluidic chip is 50 mm × 50 mm. In order to simulate formation with different degrees of fracture development, the fracture sizes of the three kinds of micromodels are 200−300 μm, 100−200 μm, and 50−100 μm, respectively, and the number of fractures decreases successively. The throat sizes of these three types of micromodels are correspondingly 15−20 μm, 8−12 μm, and 4−6 μm, respectively. To study the law of different injection methods, a micromodel with two inlets and two outlets was designed and fabricated as shown in Figure 1d. The morphology and size of pores, throats, and fractures in this micromodel was the same as that shown in Figure 1a.

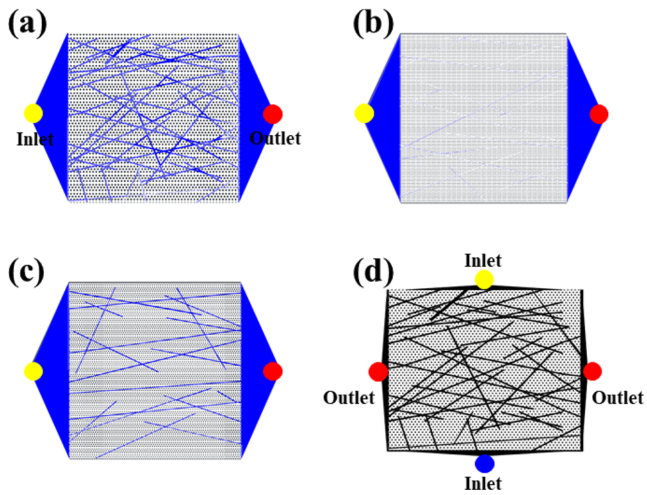

Figure 1. Schematic diagrams of microfluidic chips with one inlet and one outlet, representing formation with rich fractures (a), poor fractures (b), and medium number fractures (c) and a microfluidic chip with two inlets and two outlets (d), representing formation with rich fractures.

2.2.2. Experiments of Gas Injection to Displace Oil in Micromodel. As for gas injection to displace oil in the actual reservoirs, there are various methods of gas injection, such as gas injection from the edge of the oil formation, gas injection from the top of the oil formation, gas injection from the edge of the oil formation accompanied by water injection from the bottom of the oil formation, etc. In order to investigate the oil displacement behaviors of these three gas injection methods, the corresponding three parallel experiments were conducted. Figure 2 shows the schematic diagrams of these types of gas injection methods and corresponding physical pictures of real micromodels.

Before all of the experiments, the porous media were vacuumed and were full of water. And then, the oil was injected into the micromodel to saturate it until no water flowed out. During the first experiment, the chip was placed horizontally, as shown in Figure 2b. Then, the gas was injected from the inlet, and the produced fluid flowed out through the outlet. The injection rate was 0.01 mL/min. This experiment was employed to simulate gas injection from the edge of the oil formation. During the second experiment, the micromodel was placed vertically, and then the gas was injected through the inlet at the top of the micromodel. The produced fluid flowed out through the outlet at the bottom of the micromodel. The injection rate was 0.01 mL/min. This experiment was employed to simulate gas injection from the top of the oil formation. During the third experiment, the micromodel was placed vertically, and then the gas was injected through the inlet at the top of the micromodel, while the water was injected

https://doi.org/10.1021/acsomega.2c02390
ACS Omega 2022, 7, 27382−27389

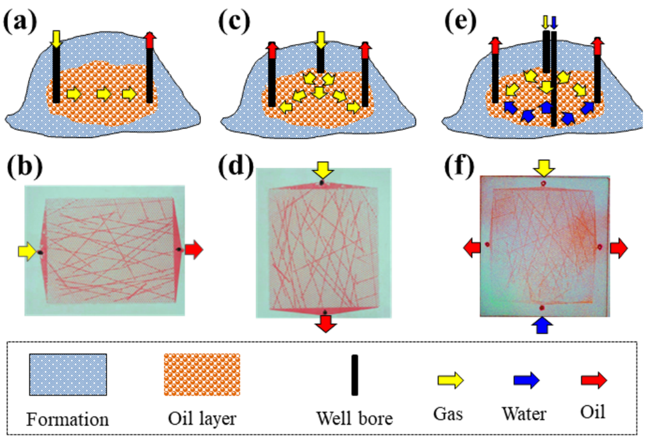

Figure 2. Schematic diagrams of gas injection from the edge of the oil formation (a), gas injection from the top of the oil formation (b), and gas injection from the top of the oil formation and water injection from the bottom of the oil formation (c) and the corresponding injection methods (b, d, and f) in real micromodels.

through the inlet at the bottom of the micromodel. And the produced fluid flowed out through the outlets on either side of the micromodel. The injection rate of gas and water was 0.005 mL/min. This experiment was employed to simulate gas injection from the top of the oil formation accompanied by water injection from the bottom of the oil formation. The microscopic pictures were recorded by a high-resolution microscope to observe the flow behaviors of gas and oil in porous media. After the experiments, the pores and throats were flushed by petroleum ether, ethanol, deionized water, and nitrogen gas in turn. Finally, the chip was dried at a constant high temperature of 60 °C for 12 h.

3. RESULTS AND DISCUSSION

3.1. Gas Injection from the Edge of Porous Media.

The sweep efficiency and oil displacement efficiency of the gas injection from the edge of porous media is shown in Figure 3. Figure 3a and b showed that, as more gas was injected, the swept area became larger and the oil production increased until the injection volume reached 8 PV. Whether it is the sweep efficiency or the oil displacement efficiency, the results showed that the porous media with rich fractures kept the highest value and the porous media with poor fractures kept the lowest value during the whole process. The porous media with rich fractures represent oil formation with well-developed fractures, high oil content, and high permeability. In the process of gas flooding, the resistance is small and able to spread to the distant pores and throats. Moreover, this phenomenon is also reflected in the sweep efficiency and oil displacement efficiency in areas of fractures and pores and throats. Due to the good connectivity and width of fractures, the flooding effect of fractures was better than those of pores and throats, as shown in Figure 3c and d. Under the method of gas injection from the edge of porous media, the overall sweep efficiency was at a relatively

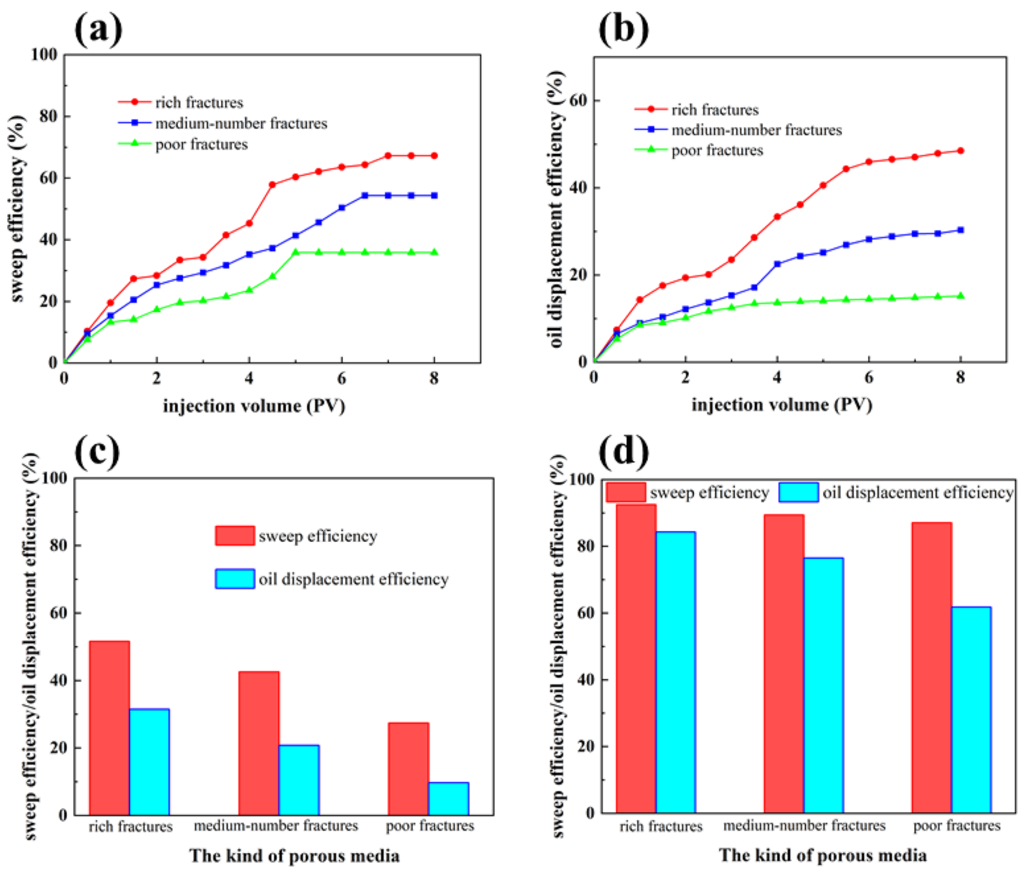

Figure 3. Cumulative sweep efficiency (a) and oil displacement efficiency (b) in different kinds of porous media as a function of gas injection volume. The sweep efficiency and oil displacement efficiency of pores and throats (c) and fractures (d) in different kinds of porous media after gas injection from the edge of porous media.

https://doi.org/10.1021/acsomega.2c02390
ACS Omega 2022, 7, 27382−27389

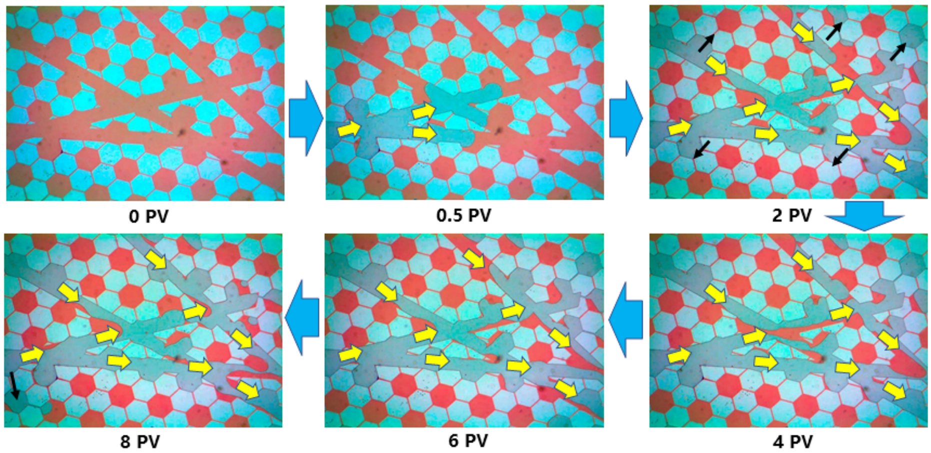

Figure 4. Displacement process of oil in fractures, pores, and throats during gas injection from the edge of porous media in a microfluidic chip with rich fractures.

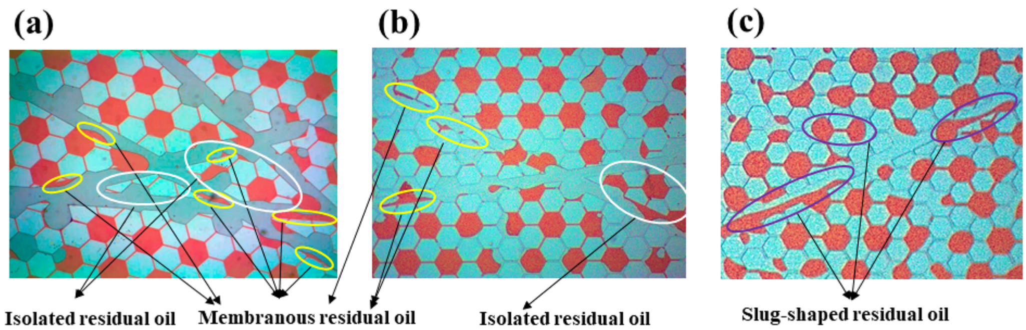

Figure 5. Morphology of residual oil in porous media after gas injection from the edge of porous media in microfluidic chips with rich fractures (a), medium-number fractures (b), and poor fractures (c).

low level, and there was high risk of gas channeling in areas of fractures.

It is found through experiments that the activation behaviors of oil in three porous media are similar, so the gas injection from the edge of porous media with rich fractures is mainly analyzed as shown in Figure 4. In the early stage of gas injection (<0.5 PV), the oil in fractures was displaced first, with a fast speed and a rapid increase in oil production. In the middle stage of gas injection (0.5−6 PV), more oil in fractures was displaced, and at the same time the oil in a large number of pores and throats around the fractures was displaced, resulting in a relatively higher peak oil production. In the later stage of gas injection (6−8 PV), a large amount of gas flowed along fractures forming gas channeling, resulting in a large decrease in displaced oil and a rapid decline in oil production. The fracture is wider than the pores and throats, so the flow resistance of gas in the fracture is lower, causing the initial gas to flow along the fracture first, displacing the oil in the fracture region. Due to the low density and high flowability, a part of subsequent gas could invade into the tight pores and throats although they are narrow channels under behaviors such as imbibition by virtue of low capillary resistance of gas. The oil in pores and throats could be partially displaced by the gas. Therefore, the gas invades the fractures first and then invades the tight pores and throats to activate and displace the oil.

The morphology of residual oil in porous media after gas injection from the edge of porous media with rich fractures, medium-number fractures, and poor fractures is shown in Figure 5a−c, respectively. In porous media with rich fractures, the formation of residual oil in swept areas was mainly isolated residual oil and membranous residual oil. The membranous residual oil refers to the residual oil attached to the wall surface of fractures and the corner of pores. The isolated residual oil refers to the residual oil in pores and throats separated by fractures. The formation of residual oil in porous media with medium-number fractures was similar to that of the porous media with rich fractures, involving two types of residual oil: isolated residual oil and membranous residual oil. However, the distribution of residual oil in porous media with medium-number fractures was more correlated with the location of fractures, which was caused by the sparsity of fractures. The residual oil in areas without fractures was distributed continuously. In porous media with poor fractures, the formation of residual oil in swept areas was mainly slug-shaped residual oil. The reason for the formation of slug-shaped residual oil was that the gas phase was cut off by the oil and the residual oil was displayed as slug-shaped in fractures. Because of the existence of high capillary force, it is difficult for gas to enter the small pores and throats, and then it is difficult to effectively displace the oil inside by gas.

3.2. Gas Injection from the Top of Porous Media. To inhibit gas channeling and thus enhance oil recovery, gas injection from the top of porous media was studied, which is also considered to be an effective method for developing some tight reservoirs with fractures. The sweep efficiency and oil displacement efficiency of gas injection from the top of porous media is shown in Figure 6. Compared with gas injection from the edge of porous media, the overall sweep efficiency of gas

https://doi.org/10.1021/acsomega.2c02390
ACS Omega 2022, 7, 27382−27389

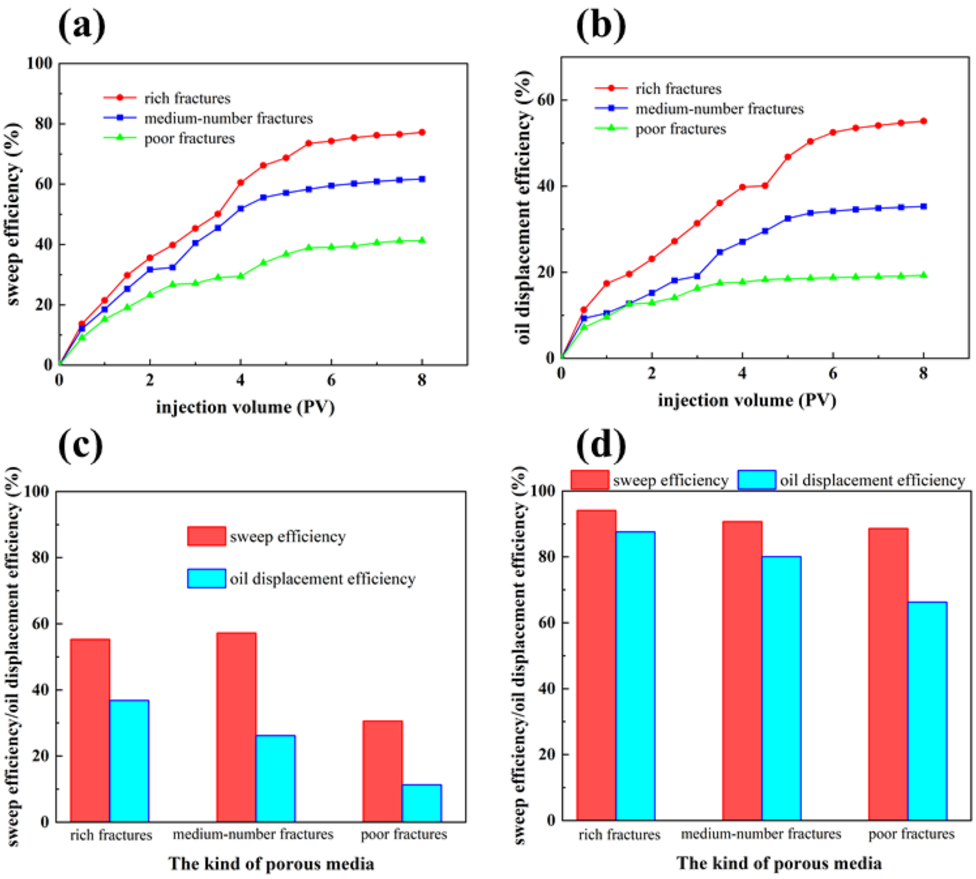

Figure 6. Cumulative sweep efficiency (a) and oil displacement efficiency (b) in different kinds of porous media as a function of gas injection volume. The sweep efficiency and oil displacement efficiency of pores and throats (c) and fractures (d) in different kinds of porous media after gas injection from the top of porous media.

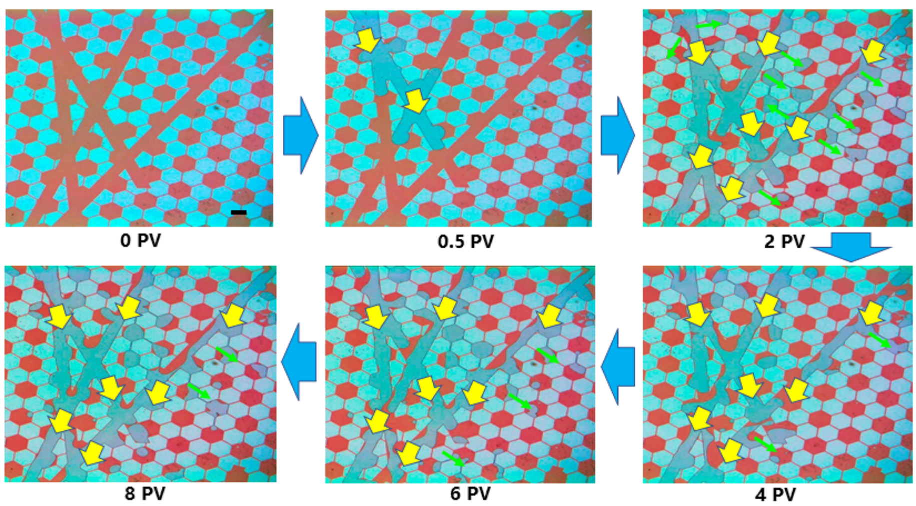

Figure 7. Displacement process of oil in fractures, pores, and throats during gas injection from the top of porous media in a microfluidic chip with rich fractures.

injection from the top of porous media increased about 5.4% to 9.9%, and the overall oil displacement efficiency increased about 4.1% to 6.6%. Additionally, gas channeling was abated due to upward gas flow caused by gravity, and thus the sweep efficiency and oil displacement efficiency of pores and throats as well as fractures were improved on average by approximately 7.2%, 4.1%, 1.5%, and 3.8%, respectively, as shown in Figure 6d. After gas channeling was inhibited, displacement of residual oil in pores and throats became more significant.

According to the behavior of gas injection from the top of porous media, the sequence of gas flooding was similar to gas injection from the edge of porous media, as shown in Figure 7. In the early stage of gas injection (<0.5 PV), the oil in fractures was displaced first. In the middle stage of gas injection (0.5−4 PV), with the displacement of oil in fractures, more oil in a

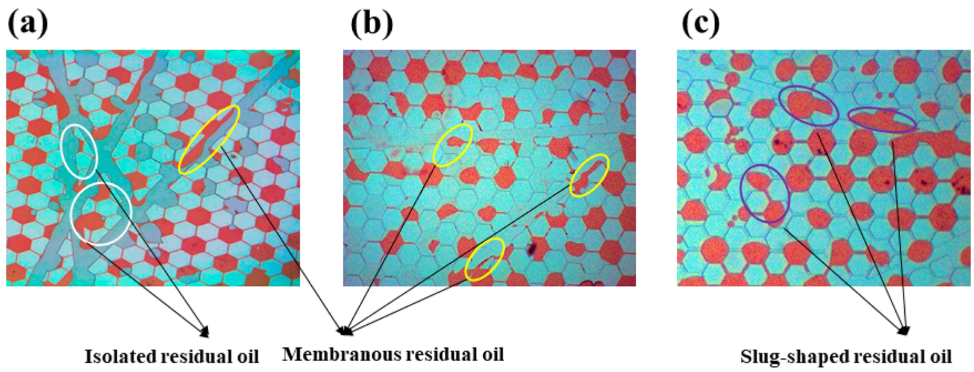

Figure 8. Morphology of residual oil in porous media after gas injection from the top of porous media in microfluidic chips with rich fractures (a), medium-number fractures, (b) and poor fractures (c).

large number of pores and throats around the fractures was displaced. In the later stage of gas injection (4−8 PV), gas channeling formed, and there was a large decrease in oil production. Although the oil recovery was improved when the gas injection from the top was employed, gas channeling was still serious, and Figure 8 shows that no matter what kind of porous media, there was still a large amount of residual oil left after gas flooding.

3.3. Simultaneous Injection of Gas and Water from the Top of Porous Media and the Bottom of Porous Media, Respectively. Simultaneous injection of gas and water from the top of porous media and the bottom of porous media, respectively, was studied to enhance the oil recovery of gas flooding. According to the displacement results of simultaneous injection of gas and water from the top of porous media and the bottom of porous media, respectively, shown in Figure 9, all areas of fractures were swept and the oil

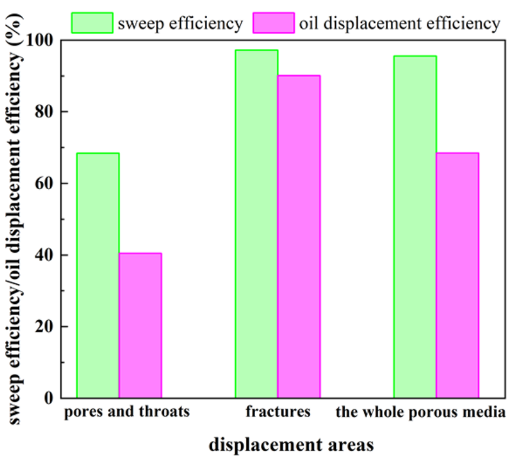

Figure 9. Sweep efficiency and oil displacement efficiency of pores and throats, fractures, and the whole porous media in porous media with rich fractures after simultaneous injection of gas and water from the top of porous media and the bottom of porous media, respectively.

in pores and throats around fractures was started and displaced when the injection volume of gas was 4 PV. When 8 PV gas was injected into porous media, the swept area was further expanded, and the oil recovery reached near the top. Simultaneous injection of gas and water from different locations significantly improved the oil recovery. Compared with the gas injection from the top of porous media, this injection method displayed more effective displacement of oil. The overall sweep efficiency and the overall oil displacement efficiency increased about 18.4% and 13.4%, respectively. This suggested that the combining gas flooding and water flooding showed an optimal enhanced oil recovery effect compared with the gas injection. Simultaneous injection of gas and water from the top of porous media and the bottom of porous media, respectively, is an optimized enhanced oil recovery method.

The better displacement effect of the combining gas and water injection can be included for three reasons. It can be seen from microscopic displacement images shown in Figure 10. First, gas can invade deep pores and throats that are difficult for water to enter, as shown in Figure 10a. Second, compared with gas, the viscosity of water is higher, and thus the water shows a relatively smaller mobility. Therefore, water flooding sweeps a larger area than pure gas flooding. Moreover, in gas−water mixing regions, two-phase flow resistance is larger than single phase, which inhibits channeling and increases the swept range. It is suggested to inject gas from a higher location and inject water from a lower location to enhance the oil recovery.

4. CONCLUSIONS

In this study, enhanced oil recovery methods for gas injection of fractured reservoirs were explored by microfluidic technology. The primary conclusions drawn from this study are summarized as follows.

(1) In the process of gas injection, there are three stages of gas displacing oil. In the early stage of gas flooding, the oil in fractures was quickly displaced first. In the middle stage of gas flooding, more oil in fractures was displaced, and at the same time the oil in pores and throats around the fractures was displaced. In the later stage of gas flooding, gas channeling mainly occurred in fractures, and very little oil was displaced out OF the porous media.

(2) The sweep efficiency and oil displacement efficiency showed a tendency of increasing first and then stabilizing. The sweep efficiency and oil displacement efficiency of fractures were much higher than those of pores and throats. And the channeling inhibition ability of gas injection from the top of porous media was more prominent, which was beneficial to delaying gas channeling occurrence.

(3) Simultaneous injection of gas and water from the top of porous media and the bottom of porous media, respectively, showed an optimal enhanced oil recovery effect among these three injection methods, which could be attributed to three main reasons. First, gas can invade deep and small pores and

https://doi.org/10.1021/acsomega.2c02390
ACS Omega 2022, 7, 27382−27389

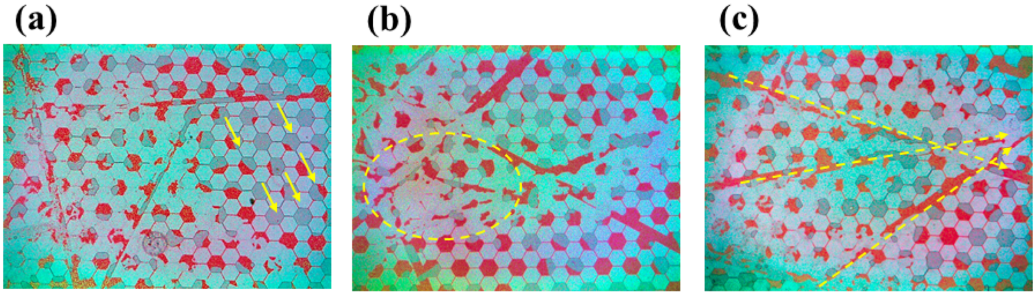

Figure 10. Oil was displaced by gas (a), water (b), and the mixture of gas and water (c) during the oil displacement by simultaneous injection of gas and water from the top of porous media and the bottom of porous media, respectively.

throats that are difficult for water to sweep. Second, the viscosity of water is higher than that of gas, endowing water a relatively smaller mobility to sweep a larger area than pure gas flooding. Third, the channeling in the gas−liquid two-phase mixing region was inhibited more obviously

(4) Compared with single phase flooding, the method of gas injection from the top and water injection from the bottom inhibits the channeling of gas more effectively in fractured reservoirs. The overall sweep efficiency and the overall oil displacement efficiency increased about 18.4% and 13.4%, respectively.

AUTHOR INFORMATION

Corresponding Author

Kang Xiao − *Research Institute of Petroleum Exploration and Development, Beijing, China 100083;* orcid.org/0000-0003-2939-2864; Email: xiaokang870224@petrochina.com.cn

Authors

Xiangling Li − *Research Institute of Petroleum Exploration and Development, Beijing, China 100083*
Ruifeng Wang − *Research Institute of Petroleum Exploration and Development, Beijing, China 100083*
Xianbing Li − *Research Institute of Petroleum Exploration and Development, Beijing, China 100083*

Complete contact information is available at:
https://pubs.acs.org/10.1021/acsomega.2c02390

Author Contributions

X.L. performed conceptualization, methodology. K.X. performed conceptualization, methodology, writing of the original draft, review, and editing. R.W. performed writing, review, and editing. X.L. performed investigation.

Notes

The authors declare no competing financial interest.

ACKNOWLEDGMENTS

This study was supported by the Scientific Research and Technology Development Project of CNPC (NO.2018D-4407 and NO.2021DJ3203).

NOMENCLATURE

LFNMR = low-field nuclear magnetic resonance
PV = pore volumes

REFERENCES

(1) Miskimins, J. L. Design and life-cycle considerations for unconventional reservoir wells. *SPE Prod. Oper.* **2009**, *24* (02), 353−359.

(2) Wang, Y.; Shang, Q.; Zhou, L.; Jiao, Z. Utilizing macroscopic areal permeability heterogeneity to enhance the effect of CO_2 flooding in tight sandstone reservoirs in the Ordos Basin. *J. Pet. Sci. Eng.* **2021**, *196*, 107633.

(3) Li, X.; Yue, X.; Zou, J.; Yan, R. Effect of in-situ emulsification of surfactant on the enhanced oil recovery in low-permeability reservoirs. *Colloids Surf., A* **2022**, *634*, 127991.

(4) You, Q.; Wang, H.; Zhang, Y.; Liu, Y.; Fang, J.; Dai, C. Experimental study on spontaneous imbibition of recycled fracturing flow-back fluid to enhance oil recovery in low permeability sandstone reservoirs. *J. Pet. Sci. Eng.* **2018**, *166*, 375−380.

(5) Yang, P.; Guo, H.; Yang, D. Determination of residual oil distribution during waterflooding in tight oil formations with NMR relaxometry measurements. *Energy Fuels* **2013**, *27* (10), 5750−5756.

(6) Wu, Y.; Chen, W.; Dai, C.; Huang, Y.; Li, H.; Zhao, M.; He, L.; Jiao, B. Reducing surfactant adsorption on rock by silica nanoparticles for enhanced oil recovery. *J. Pet. Sci. Eng.* **2017**, *153*, 283−287.

(7) Lin, R.; Yu, Z.; Zhao, J.; Dai, C.; Sun, Y.; Ren, L.; Xie, M. Experimental evaluation of tight sandstones reservoir flow characteristics under CO_2−Brine−Rock multiphase interactions: A case study in the Chang 6 layer, Ordos Basin, China. *Fuel* **2022**, *309*, 122167.

(8) Tang, W.; Sheng, J. J. Huff-n-puff gas injection or gas flooding in tight oil reservoirs? *J. Pet. Sci. Eng.* **2022**, *208*, 109725.

(9) Chen, L.; Ji, H.; Dou, L.; Du, Y.; Xu, Z.; Zhang, L.; Yang, X.; Fu, S. The characteristics of source rock and hydrocarbon charging time of Precambrian granite reservoirs in the Bongor Basin, Chad. *Mar. Petrol. Geol.* **2018**, *97*, 323−338.

(10) Dong, W.; Jiao, J.; Xie, S.; Lyu, C.; Cui, G.; Meng, J. Cumulative production curve method for the quantitative evaluation on the effect of oilfield development measures: A case study of the nitrogen injection pilot in Yanling oilfield, Bohai Bay Basin. *Petrol. Explor. Dev.* **2016**, *43* (4), 672−678.

(11) Cuong, T. X.; Warren, J. Bach ho field, a fractured granitic basement reservoir, Cuu Long Basin, offshore SE Vietnam: A "buried-hill" play. *J. Pet. Geol.* **2009**, *32* (2), 129−156.

(12) Hill, B.; Hovorka, S.; Melzer, S. Geologic carbon storage through enhanced oil recovery. *Energy Procedia* **2013**, *37*, 6808−6830.

(13) Qin, J.; Han, H.; Liu, X. Application and enlightenment of carbon dioxide flooding in the United States of America. *Petrol. Explor. Dev.* **2015**, *42* (2), 232−240.

(14) Li, X. j.; Hu, S. y.; Cheng, K. M. Suggestions from the development of fractured shale gas in North America. *Petrol. Explor. Dev.* **2007**, *34* (4), 392.

(15) Sheng, J. J.; Chen, K. Evaluation of the EOR potential of gas and water injection in shale oil reservoirs. *J. Unconv. Oil Gas Resour.* **2014**, *5*, 1−9.

(16) Jin, L.; Hawthorne, S.; Sorensen, J.; Pekot, L.; Kurz, B.; Smith, S.; Heebink, L.; Herdegen, V.; Bosshart, N.; Torres, J.; Dalkhaa, C.; Peterson, K.; Gorecki, C.; Steadman, E.; Harju, J. Advancing CO_2 enhanced oil recovery and storage in unconventional oil play—

https://doi.org/10.1021/acsomega.2c02390
ACS Omega 2022, 7, 27382−27389

experimental studies on Bakken shales. *Applied Energy* **2017**, *208*, 171−183.
(17) Berkowitz, B. Characterizing flow and transport in fractured geological media: A review. *Adv. water resour.* **2002**, *25* (8−12), 861−884.
(18) Zhang, X.; Huang, Z.; Lei, Q.; Yao, J.; Gong, L.; Sun, S.; Li, Y. Connectivity, permeability and flow channelization in fractured karst reservoirs: A numerical investigation based on a two-dimensional discrete fracture-cave network model. *Adv. water resour.* **2022**, *161*, 104142.
(19) Wei, C.; Cheng, S.; Wang, Y.; Shi, W.; Li, J.; Zhang, J.; Yu, H. Practical pressure-transient analysis solutions for a well intercepted by finite conductivity vertical fracture in naturally fractured reservoirs. *J. Pet. Sci. Eng.* **2021**, *204*, 108768.
(20) Ye, T.; Niu, C.; Wei, A. Characteristics and genetic mechanism of large granitic buried-hill reservoir, a case study from PengLai oil field of Bohai Bay Basin, north China. *J. Pet. Sci. Eng.* **2020**, *189*, 106988.
(21) Carvalho, I. d. S.; Mendes, J. C.; Costa, T. The role of fracturing and mineralogical alteration of basement gneiss in the oil exhsudation in the Sousa Basin (Lower Cretaceous), Northeastern Brazil. *J. S. Am. Earth Sci.* **2013**, *47*, 47−54.
(22) Huang, J.; Tan, X.; Cheng, C.; Li, Z.; Ma, L.; Zhang, H.; Wu, Y. Structural features of weathering crust of granitic basement rock and its petroleum geological significance: A case study of Basement weathering crust of Dongping Area in Qaidam Basin. *Earth Sci.* **2016**, *41*, 2041−2060.
(23) Hasan, M.; Shang, Y.; Jin, W. Delineation of weathered/fracture zones for aquifer potential using an integrated geophysical approach: A case study from South China. *J. Appl. Geophysics* **2018**, *157*, 47−60.
(24) Ishibashi, T.; Watanabe, N.; Tamagawa, T.; Tsuchiya, N. Three-dimensional channeling flow within subsurface rock fracture networks suggested via fluid flow analysis in the yufutsu fractured oil/gas reservoir. *J. Pet. Sci. Eng.* **2019**, *178*, 838−851.
(25) Huang, X.; Zhang, L.; Zhang, R.; Chen, X.; Zhao, Y.; Yuan, S. Numerical simulation of gas-liquid two-phase flow in the micro-fracture networks in fractured reservoirs. *J. Nat. Gas Sci. Eng.* **2021**, *94*, 104101.
(26) Pu, W. f.; Du, D. j.; Fan, H. c.; Chen, B. w.; Yuan, C. D.; Varfolomeev, M. A. CO_2-responsive preformed gel particles with interpenetrating networks for controlling CO_2 breakthrough in tight reservoirs. *Colloids Surf., A* **2021**, *613*, 126065.
(27) Zhao, F.; Wang, P.; Huang, S.; Hao, H.; Zhang, M.; Lu, G. Performance and applicable limits of multi-stage gas channeling control system for CO_2 flooding in ultra-low permeability reservoirs. *J. Pet. Sci. Eng.* **2020**, *192*, 107336.
(28) Conn, C. A.; Ma, K.; Hirasaki, G. J.; Biswal, S. L. Visualizing oil displacement with foam in a microfluidic device with permeability contrast. *Lab Chip* **2014**, *14* (20), 3968−77.
(29) Bai, H.; Zhang, Q.; Li, Z.; Li, B.; Zhu, D.; Zhang, L.; Lv, G. Effect of fracture on production characteristics and oil distribution during CO_2 huff-n-puff under tight and low-permeability conditions. *Fuel* **2019**, *246*, 117−125.
(30) Chen, H.; Li, H.; Li, Z.; Li, S.; Wang, Y.; Wang, J.; Li, B. Effects of matrix permeability and fracture on production characteristics and residual oil distribution during flue gas flooding in low permeability/tight reservoirs. *J. Pet. Sci. Eng.* **2020**, *195*, 107813.
(31) Zhang, Y.; Gao, M.; You, Q.; Fan, H.; Li, W.; Liu, Y.; Fang, J.; Zhao, G.; Jin, Z.; Dai, C. Smart mobility control agent for enhanced oil recovery during CO_2 flooding in ultra-low permeability reservoirs. *Fuel* **2019**, *241*, 442−450.